http://dx.doi.org/10.5935/0103-5053.20160080

J. Braz. Chem. Soc., Vol. 27, No. 11, 1949-1959, 2016.
Printed in Brazil - ©2016 Sociedade Brasileira de Química
0103 - 5053 $6.00+0.00

Article

Bacterial Cellulose Membranes as a Potential Drug Delivery System for Photodynamic Therapy of Skin Cancer

Maristela F. S. Peres,[a,#] Karina Nigoghossian,[b,#] Fernando L. Primo,[a,c] Sybele Saska,[b] Ticiana S. O. Capote,[d] Raquel M. S. Caminaga,[d] Younes Messaddeq,[b] Sidney J. L. Ribeiro[b] and Antonio C. Tedesco*[,a]

[a]*Centro de Nanotecnologia, Engenharia Tecidual e Fotoprocessos Voltado a Saúde, Grupo de Fotobiologia e Fotomedicina, Departamento de Química, Faculdade de Filosofia, Ciências e Letras de Ribeirão Preto (FFCLRP-DQ), Universidade de São Paulo, Campus Ribeirão Preto, 14040-901 Ribeirão Preto-SP, Brazil*

[b]*Instituto de Química, Universidade Estadual Paulista "Júlio de Mesquita Filho" (UNESP), CP 355, 14801-970 Araraquara-SP, Brazil*

[c]*Departamento de Bioprocessos e Biotecnologia, Faculdade de Ciências Farmacêuticas, Universidade Estadual Paulista "Júlio de Mesquita Filho" (UNESP), 14801-902 Araraquara-SP, Brazil*

[d]*Departamento de Morfologia, Faculdade de Odontologia, Universidade Estadual Paulista "Júlio de Mesquita Filho" (UNESP), 14801-903 Araraquara-SP, Brazil*

The development of drug delivery systems for photodynamic therapy (PDT) is increasingly demanded due to the hydrophobicity presented by most of photosensitizers molecules. Bacterial cellulose (BC), a highly pure cellulose produced by bacteria, possesses the essential features for applications in drug delivery systems, such as large surface area and excellent loading capacity. BC membranes prepared containing a photosensitizer, chloroaluminum phthalocyanine (ClAlPc), were tested aiming applications as a drug delivery system for PDT skin cancer protocols. BC membranes production was optimized regarding thickness and optical transmission. Thinner membranes lead to higher relative incorporation efficiencies. Skin permeation and retention *in vitro* tests were performed by using pig's ears as a skin model. ClAlPc was retained at stratum corneum and epidermis/dermis, showing adequate properties for topical administration of ClAlPc. Photophysical studies showed that singlet oxygen production was not affected for ClAlPc compartmentalized in the BC array. BC-ClAlPc membranes did not present cytotoxic effects *in vitro*.

Keywords: bacterial cellulose, phthalocyanine, drug delivery system, photodynamic therapy

Introduction

A variety of new approaches and therapeutic protocols has been emerging in the last years as a consequence of the progresses in the field of applied nanobiotechnology to treat a huge spectrum of diseases, through improved targeting or delivery of the therapeutic agent. In the case of application for cancer therapeutics, these innovative technologies tend to be less invasive and more effective when compared with the most conventional antitumor treatment techniques: surgery, radiotherapy and chemotherapy.[1-3] Photodynamic therapy (PDT) has been focus of intense research during the last decades as an emerging therapeutic modality. Despite the fact of being a novel technique, PDT is a well-established procedure mainly used in the treatment of neoplastic and non-neoplastic diseases.[4] This therapy is focused mainly in skin cancer treatment, from early stage until melanoma one (there is no indication for the use of this therapy to treat melanoma). PDT is already used as a clinical tool for treating tumors and a considerable number of pathological conditions, such as arthritis, skin disorders and many other non-oncological diseases.[5-8] The technique is based on the injection, ingestion, or topical application of photosensitizer drugs (usually obtained from natural or

*e-mail: atedesco@usp.br
#Maristela de F. S. Peres and Karina Nigoghossian contributed equally to this paper.

synthetic sources, in the presence of a specific drug delivery system) followed by visible light activation.[9] The classical photosensitizers are chemical compounds, which absorb visible light in a specific wavelength. Upon irradiation, the photosensitizer is promoted from its ground singlet state to its triplet excited state followed by reactions that occurs in a complex mechanistic pathway through classical photochemical reactions,[10] leading to the production of reactive oxygen species (ROS), of which singlet oxygen is one of the main active species in photodynamic processes.

Most of the photosensitizers used in PDT present difficulty for administration in physiological environment due to their hydrophobicity. Therefore, it is necessary to develop drug delivery systems capable to overcome the tendency to aggregate in aqueous media.[11] The development of new drug delivery systems based in nanobiotechnology has improved the therapeutic and toxicological properties of existing chemotherapeutic and photochemotherapeutic agents and fostered the implementation of new agents. A wide assortment of biomaterials with suitable biological properties is offered today as a potential tool to be used as a drug delivery system, but considerable attention has been drawn to the use of biocompatible polymers based ones. By combining drugs with different polymers, either synthetic or natural, it is possible to optimize pharmacokinetics and biodistribution of the agents, and, consequently efficacy and safety of therapy are improved.[12] Additionally, the polymer offers protection against enzymatic, hydrolytic and other types of chemical degradation.[13]

Polymeric release systems can be designed in many forms, including matrices or membranes in which the active ingredient is dispersed or dissolved.[14-16] The administration route, carrier formulation, release mechanism and physiochemical properties of drug molecule are determinant factors, which influence on drug release rate and thus must be considered when selecting a suitable polymer of a release device.[17] Moreover, the ideal polymers for the development of dry delivery systems should be chemically inert to the drug action and present appropriate physical features.[18]

Bacterial cellulose (BC) is a polysaccharide of glucose produced by *Gluconacetobacter* sp. that is superior to plant cellulose due to its purity and nano-morphology. BC presents high water-holding capacity, large surface area, and high crystallinity, besides being renewable, biocompatible and biodegradable.[19] The incorporation of organic/inorganic compounds in its structure is possible due to the network of ribbon-shaped nanosized cellulose fibrils and the high presence of water. A number of studies in the literature report the successful use of BC membranes in biomedical applications[20] and, more specifically, drug delivery systems[21] due to their unique physical and mechanical properties.[22] Such membranes are particularly advantageous in topical or transdermal drug delivery systems, as they have the ability to absorb exudates and adhere to irregular skin surfaces, such as the oral mucosa.[23-26] Moreover, a previous study reported the good skin tolerance of BC membranes.[27] As the majority of transdermal patches are manufactured by superimposing different materials, a system composed of fewer or even a single layer, such as a BC film, could simplify the preparation procedure and lower production costs.[28] Recently, our group has reported a system based on BC membranes incorporated with the photosensitizer chloroaluminum phthalocyanine (ClAlPc) and luminescent upconversion nanoparticles, which emits light at the wavelength range of ClAlPc absorption under infrared irradiation, within the biological transparency window.[29] Chitosan, which is chemically related to cellulose and plant cellulose nanocrystals, has been studied by Schmitt *et al.*[30] and Drogat *et al.*[31] in photodynamic therapy. In view of these facts, the development of new delivery systems that can efficiently deliver ClAlPc could enable its clinical use for topical PDT.

The aim of the present study was to show the feasibility of bacterial cellulose as a potential drug delivery system for photodynamic therapy. The BC-ClAlPc membranes were evaluated regarding the incorporation efficiency of photosensitizer and *in vitro* diffusion studies with Franz cells. The BC-ClAlPc membranes were tested as a setup to activate photoprocesses useful for treat neoplastic and non-neoplastic diseases susceptible to the photoactivation process. The cytotoxicity potential of BC-ClAlPc was evaluated aiming a safe use in humans.

Experimental

Microorganisms

The strains used were *Acetobacter xylinum* (ATCC 23760) and other isolated in the laboratory identified by Centro Pluridisciplinar de Pesquisas Químicas, Biológicas e Agrícolas (CPQBA), Universidade Estadual de Campinas (UNICAMP) as *Gluconacetobacter* sp. (GL). BC obtained from each microorganism were produced in two different stages of growth, in order to vary the thickness of the membranes: ATCC (2 and 3 days) and GL (1 and 3 days).

Chemicals

Glucose, yeast extract, potassium phosphate monobasic anhydrous, magnesium sulphate heptahydrate, and ethanol, all of analytical grade, were used for the

microbiological culture media. ClAlPc, dimethyl sulfoxide (DMSO), phosphate buffer saline solution (PBS), sodium 3'-[1-(phenylaminocarbonyl)-3,4-tetrazolium]-bis (4-methoxy-6-nitro) benzene sulfonic acid hydrate (yellow tetrazolium salt XTT), cell culture medium Ham's F-10 (HAM-F10):Dulbecco's modified Eagle's (DMEN), 1:1 and doxorubicin were purchased from Sigma-Aldrich (St. Louis, MO, USA). Fetal bovine serum (FBS) and DMEM medium without phenol red were purchased from Cultilab (Campinas, SP, Brazil). XTT:electron solution 50:1 cell proliferation kit II (XTT) was acquired from Roche Molecular Biochemicals (Basel, Switzerland).

Bacterial cellulose production

The BC membranes were produced by growing the bacteria at 30 °C for 24 h in liquid medium under static conditions. Culture medium was composed of 50 g L^{-1} glucose, 4 g L^{-1} yeast extract, 2 g L^{-1} potassium phosphate monobasic anhydrous, 0.73 g L^{-1} magnesium sulphate heptahydrate, and 20 g L^{-1} ethanol.[32] After this period, the flask was vigorously agitated and 10% of the culture media was withdrawn and inoculated into a new liquid production medium at 30 °C over different periods of time (24, 48 and 72 h).

Bacterial cellulose purification

After the incubation time, BC membranes were withdrawn from the culture medium and treated with a 0.1 mol L^{-1} NaOH solution, at 80 °C, for 30 min to eliminate all attached cells. Then, the membranes were washed with distilled water to remove components of the culture media and other residues until its whitening and reaching pH 7.0. BC membranes were dried at 30 °C and then stored in a desiccator. Measurements of the thickness of the membranes were performed in a Formtracer profilometer, model SV-CS25 (Mitutoyo, Kawasaki, Japan).

Chloroaluminum phthalocyanine (ClAlPc) in bacterial cellulose membranes

The BC wet membranes (5 × 5 cm) were weighed. Moderate pressure was applied to the surface of the membranes to remove water until the mass loss of 50%. The drained BC membranes were then soaked for 5 h in ClAlPc solutions in ethanol at concentrations of 1, 5 and 10 μmol L^{-1}. The membranes were dried at 28 °C in a ventilated oven for 6 h.

To facilitate the understanding of the results, it is important to highlight that BC refers to bacterial cellulose membranes and BC-ClAlPc refers to the bacterial cellulose membranes incorporated with the photosensitizer ClAlPc. The samples are referred according to three factors: (*i*) the strains from which membranes were produced: ATCC (A) or GL (G); (*ii*) the stages of growth: one, two or three days (1d, 2d and 3d, respectively); (*iii*) when applicable, the theoretical concentrations of ClAlPc (1, 5 and 10 μmol L^{-1}) are indicated by the numbers 1, 5 and 10 at the end of samples names. Table 1 presents the sample names according to these variables.

Table 1. List of sample names and corresponding variables

Sample	Strain	Stage of growth / day	Theoretical concentration of ClAlPc / (μmol L^{-1})
G1d1	GL	1	1
A2d1	ATCC	2	1
G3d1	GL	3	1
A3d1	ATCC	3	1
G1d5	GL	1	5
A2d5	ATCC	2	5
G1d10	GL	1	10
A2d10	ATCC	2	10

ATCC: *Acetobacter xylinum*; ClAlPc: chloroaluminum phthalocyanine; GL: *Gluconacetobacter* sp.

The quantification of ClAlPc was carried out according to a validated methodology based in fluorescence spectroscopic technique (Spex-FluoroLog 3, Horiba Jobin Yvon, Edison, NJ, USA) with excitation at fixed wavelength (λ_{ex} 615 nm) and emission at 680 nm (slits were adjusted to 10 nm).[33]

The ClAlPc content was analyzed in two steps. Firstly, BC-ClAlPc (1 mg) was immersed in 5 mL of acetonitrile at 60 ºC for 15 min to determine the free ClAlPc content (non-incorporated drug). Subsequently, the membrane was immersed in 5 mL of acetonitrile and homogenized in an IKA Ultra-Turrax T-8 Basic (Staufen, Germany) at 11000 rpm for 5 min to quantify ClAlPc retained into BC fibers. The concentrations were obtained from a calibration standard curve. Total ClAlPc concentration corresponds to the sum of the values found in sequential steps described above. Efficiency of incorporation (EI) of the photosensitizer into BC membranes was calculated by the following equation

$$EI(\%) = \left[\frac{(\text{total ClAlPc concentration} - \text{free ClAlPc concentration})}{\text{theoretical ClAlPc concentration}}\right] \times 100 \quad (1)$$

The experiments were performed in duplicate. One-way analysis of variance (ANOVA; OriginPro 8.0, OriginLab,

Northampton, UK) was used for statistical analysis at a significance level $p < 0.05$.

Scanning electron microscopy images of BC and BC-ClAlPc surfaces were obtained with a LEO equipment model 440 (Leica, Wetzlar, Germany) with an Oxford detector. Fourier transform infrared (FTIR) spectra were obtained with a PerkinElmer Spectrum 2000 Fourier transform infrared spectrophotometer (Waltham, MA, USA) using KBr pellets. Thirty-two scans were acquired over the range 4000-370 cm^{-1} with a resolution of 2 cm^{-1}.

In vitro skin diffusion studies

PBS + ethanol 10% (v/v; 7 mL, pH 7.4) were used as the acceptor medium.[34] A calibration standard curve of ClAlPc in the acceptor medium was constructed as a reference. Aliquots of ClAlPc were added with a microsyringe (Hamilton, Ocala, FL, USA) directly in medium in a 1.0 cm quartz cell under constant stirring. The fluorescence emission spectra were determined in the range of 0.219-1.314 μg mL^{-1} (n = 10).

The skin was extracted from the dorsal surface of pig's ears, obtained directly from a slaughterhouse (Olho d'Água Ind. e Com. de Carnes Ltda., Ipuã, SP, Brazil), to be used as a model of skin. The front ear was dissected. The skins were applied in the tests *in natura.* These tissues were stored in a freezer up to a maximum of 90 days before their use in all *in vitro* procedures as an animal model. *In vitro* retention studies were carried out using the skin tissues fixed on Franz diffusion cells (1.77 cm^2 diffusion surface areas) maintained at 37 °C by a circulating water bath and stirring speed of 300 rpm. Samples were directly applied topically to the exposed area of skin. After 6, 12 and 24 h of diffusion test, the system was dismounted and the skins were carefully removed to perform the tape-stripping analyses. In this second step, the stratum corneum (SC) was extracted from the diffusion surface by using 15 standardized stripping tapes (Scotch 3M, Maplewood, MN, USA). The tape-strips were placed in 5 mL of acetonitrile in glass tubes, stored overnight and then stirred for 1 min before filtration. The remaining skin (epidermis + dermis) was cut in small pieces and added to 5 mL of acetonitrile in a tissue homogenizer, sonicated for 20 min and then centrifuged for 15 min at 5000 rpm.[35] ClAlPc amounts present in tape-strips and remaining skin (epidermis + dermis) were assayed by fluorescence standard curve. Assays were performed in three independent experiments with five replicates on each. The statistical analysis was performed using the software OriginPro 8.0 (OriginLab, Northampton, UK) by the method one-way ANOVA at a significance level $p < 0.05$.

Photophysical studies

Photophysical studies were performed to determine singlet oxygen generation. Lifetime was calculated from kinetic analysis of the mono-exponential decay for transient species obtained at 355 nm. The spectrophotometer used for time-resolved measurements was an Edinburgh analytical instruments, model FL9000CD (Livingston, UK). The source of irradiation was a pulsed Nd:YAG laser from Continuum (Surelite I-10, Continuum, Santa Clara, CA, USA) adjusted for the third harmonic (355 nm). The pulse length was 8 ns and the repetition rate was 10 Hz. The pulse energy was 15 mJ, measured by a power meter (FieldMaster, Coherent, Santa Clara, CA, USA). The decay kinetics was measured at a single wavelength using a monochromator M300 and a photomultiplier R928P from Bentham Instruments (Livingston, UK). Singlet oxygen was detected by phosphorescence emission signal at 1270 nm using a germanium photodetector of North Coast Scientific Corporation, model 823 (North Coast Scientific, LLC., Santa Rosa, CA, USA). The software provided by Edinburgh instruments (L900, Livingston, UK) was used to obtain and analyze the exponential decay curves, based on iterative algorithm Marquadt (analysis of nonlinear least squares). The BC membrane produced by ATCC with theoretical ClAlPc concentration of 5.0 μmol L^{-1} was analyzed. ClAlPc in ethanol was adopted as a reference. The experiments were done using a solution of pheophorbide A in ethanol as a standard for relative calculations.[36] The concentrations of reference solutions were adjusted based on the absorbance at 355 nm (excitation wavelength), fixed in 0.3 to avoid any internal filter effects. The measurements were performed under air-equilibrated conditions.

Cytotoxicity test

The potential cytotoxic effect of the new biomaterial obtained was evaluated by XTT assay that quantifies the cells by measuring their metabolic activity. The methodology is based on the cleavage of the yellow tetrazolium salt XTT by metabolically active cells, forming an orange formazan dye that can be measured by its absorbance at 492 nm. Thus, this conversion occurs only in viable cells due to the activity of mitochondrial dehydrogenases.[37]

The BC-ClAlPc membranes were tested using an eluate prepared according to the ISO 10993-12:2007(E), considering the surface area (6 cm^2 mL^{-1}). The membranes were immersed in culture medium HAM-F10:DMEN 1:1 in the absence of FBS at 37 ºC for 72 h under stirring (133 rpm) in an incubator (New Brunswick Excella E24 incubator shaker, Edison, NJ, USA). After 72 h, the

membranes were removed from the medium and this resulting eluate was used to carry out the treatment.

Chinese hamster ovary cells (CHO-K1) were cultured in the medium HAM-F10:DMEN 1:1 supplemented with 10% of FBS at 37 ºC and 5% of CO_2. Cells were used after the third passage. Cytotoxicity test was performed in three independent replicates. Each treatment, including positive controls (PC) and negative controls (NC), was carried out in triplicate using cell culture plates.

Cells (2×10^4) were seeded in 24-well plates in culture medium (1 mL, HAM-F10:DMEN 1:1) supplemented with 10% of FBS at 37 ºC and 5% of CO_2. After 24 h, the cells were washed with PBS, and then treated with the eluates. The cells were exposed to the eluates for 24 h. NC were cells CHO-K1 without any treatment (untreated controls), while PC were treated with doxorubicin (3 μg mL^{-1}) for 24 h.

After the treatment, the cultures were washed with PBS (250 μL) and inserted in the culture medium supplemented with FBS. After 24 h of incubation, the cells were washed with PBS (250 μL). DMEM medium without phenol red was added (1 mL), followed by 60 μL of XTT/electron solution 50:1 that remained in culture at 37 ºC for 3 h. The culture medium was then transferred to a 96-well plate, and the absorbance was measured by a microplate reader (VersaMax, Molecular Devices, Sunnyvale, CA, USA) at 492 and 690 nm. The absorbance is directly proportional to the number of viable cells in each treatment after 24 h of exposure.

For each analyzed sample, the results from three individual experiments (each one made in triplicate) were subjected to one-way ANOVA followed by Tukey's test. Dunnett's test was also applied to compare data from treated groups to the negative control. BioEstat statistical package version 5 was used (Universidade Federal do Pará, Belém, PA, Brazil) to perform the tests. Differences were considered statistically significant when $p < 0.05$.

Results and Discussion

Bacterial cellulose membranes characterization

The bacterial cellulose membranes were obtained with different characteristics regarding thickness and transparency in accordance with the bacteria strain (ATCC or GL) and the growth time (1, 2 or 3 days). The thickness of pure bacterial cellulose membranes (Figure 1) were characterized by using a profilometer. One of the goals of this work was to produce BC membranes with different characteristics to select the most appropriate for the intended application. Thickness is a structural property of the membranes that influences loading and releasing efficiency of drug into the polymeric matrix. Note that the membranes produced by ATCC (with stage of growth of 2 and 3 days, A2d and A3d) present greater values of thickness (103.2 ± 6.9 and 156.0 ± 22.4 μm) due to a greater amount of cellulose fibers present. The membranes produced by the strain GL (with stage of growth of 1 and 3 days, G1d and G3d) are thinner (thickness of 39.7 ± 5.3 and 62.2 ± 4.6 μm).

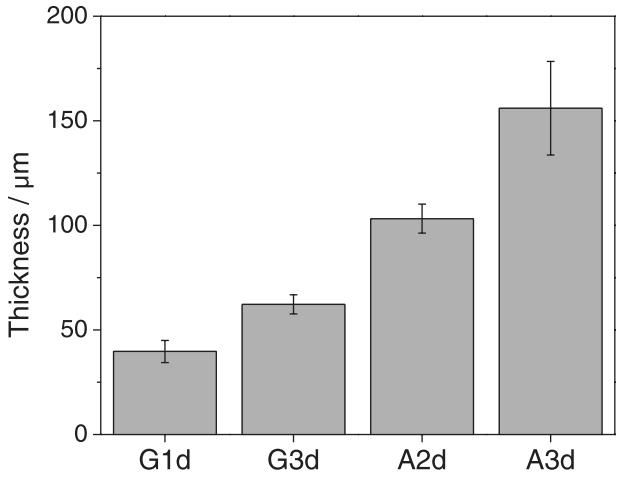

Figure 1. Thickness of pure bacterial cellulose (BC) membranes.

The electronic spectroscopy in the visible region was applied to evaluate the optical transmission of the membranes. Figure 2 shows the spectra of BC membranes, confirming the greater transparency at lesser thickness. We observed similar transparency for BCs produced by different strains. It is expected that a higher amount of fibers favors the incorporation of a greater amount of drug. The amount of fibers is improved with prolonged incubation of

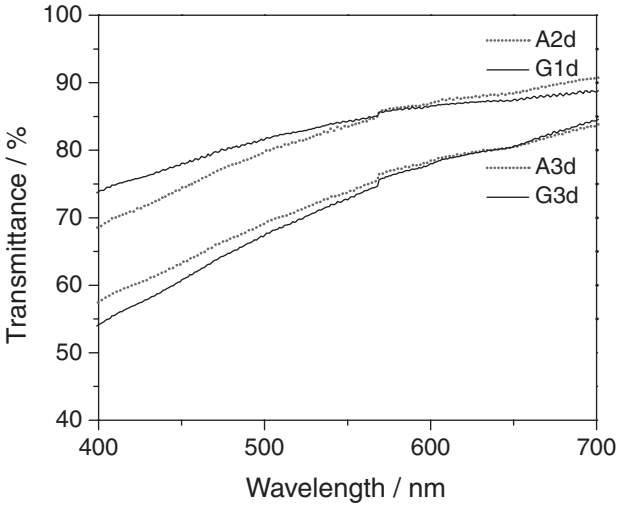

Figure 2. Optical transmission spectra of pure bacterial cellulose (BC) membranes.

the bacteria. On the other hand, thicker membranes obtained from longer cultivation have lower transparency. The highly transparent media for incorporation of the photosensitizer is favorable for the transmission of the source of light used for excitation.

ClAlPc incorporation in bacterial cellulose membranes

The strategy used here was the incorporation of ClAlPc into the bacterial cellulose membrane, for use in PDT trials for cancer treatment. The pure BC wet membrane (Figure 3a) was soaked in a solution of ClAlPc (Figure 3b) and then dried (Figure 3c). The color of the membranes turned from white to blue after incorporation of ClAlPc. The morphology was investigated by scanning electron microscope (SEM) as shown in Figure 3d. The micrographs of BC-ClAlPc showed the tridimensional fibrillar network characteristic of BC and the absence of aggregates formation, which indicated no precipitation of ClAlPc.

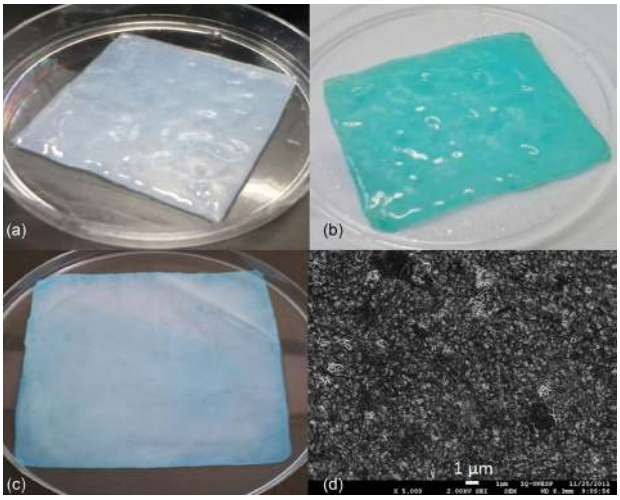

Figure 3. Photographs of pure bacterial cellulose (BC) wet membrane (a); BC- chloroaluminum phthalocyanine (ClAlPc) wet (b); dried BC-ClAlPc membrane (c); and scanning electron microscope (SEM) image of BC-ClAlPc (d).

Figure 4 displays the FTIR spectra of ClAlPc, pure BC dried membrane and BC-ClAlPc. The characteristic vibrational frequencies assigned to cellulose were observed at 3500 to 3200 cm^{-1} (OH stretching), 2908 cm^{-1} (CH stretching of CH_2 and CH_3 groups), 2700 cm^{-1} (CH_2), 1645 cm^{-1} (water OH bending), 1435 cm^{-1} (CH_2 symmetric bending), 1370 cm^{-1} (CH bending), 1160 cm^{-1} (anti-symmetric bridge C–O–C stretching), 1111 and 1056 cm^{-1} (skeletal vibrations involving C–O stretching).[19] The phthalocyanines present the following characteristic bands: at around 518 and 760 cm^{-1} (Al–N stretching), 1329 cm^{-1} (C–N–C stretching), 1121 cm^{-1} (C=C stretching of benzene rings) and 489 cm^{-1} (stretching Cl–Al).[38] The spectrum of BC-ClAlPc is basically formed by the sum of the bands present in the BC and ClAlPc spectra. The decrease in intensity of the band with a peak at 2908 cm^{-1} (CH stretching of CH_2 and CH_3 groups) on BC-ClAlPc spectrum suggests that the presence of the ClAlPc affected the cellulose groups, due to the interactions between the hydrophobic ClAlPc molecule and CH groups of cellulose, and confirms the strong interaction between the BC and ClAlPc.

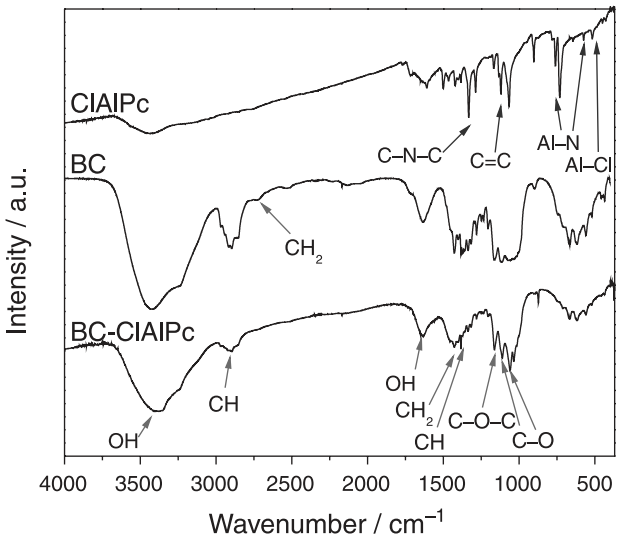

Figure 4. Fourier transform infrared (FTIR) spectra of chloroaluminum phthalocyanine (ClAlPc), dried bacterial cellulose (BC) membrane and BC-ClAlPc membrane.

The incorporation efficiency of ClAlPc from the solutions of different concentrations into membranes with different characteristics was studied. Fluorescence spectra (excitation at 615 nm) were measured after the steps of extraction of free ClAlPc in acetonitrile and homogenization of BC membranes. The ClAlPc well known emission at 680 nm, obtained under 615 nm excitation, is shown in the Figure 5a. The presence of the characteristic emission of ClAlPc confirmed the incorporation of this phthalocyanine derivative into BC fibrils.[33,39]

Figure 5b shows the ClAlPc amount retained in the fibrils (measured at homogenization step) and total ClAlPc for membranes with different theoretical concentrations (1, 5 and 10 µmol L^{-1}). These membranes were produced with the minimal time of growth stage that was enough to obtain membranes with satisfactory mechanical resistance and good transparency (that is 1 day for GL and 2 days for ATCC). The incorporation efficiencies of ClAlPc are listed in Table 2. The statistical analysis (ANOVA) confirmed a significant difference ($p > 0.05$) between the membranes. It was possible to determine an efficient and

validate quantification method for analyses of ClAlPc loaded into cellulose.[33] Studies have investigated the incorporation efficiency of ClAlPc in different bacterial cellulose membranes. A2d showed higher concentrations in steps of extraction and homogenization for all theoretical concentrations studied (1, 5 and 10 μmol L^{-1}). Figure 5b shows that, as the theoretical concentration of ClAlPc increases, the amount of ClAlPc retained in the cellulose fibers increases in a less pronounced way in respect to the total amount of incorporated drug (free + retained). Thus, membranes with lower ClAlPc theoretical concentration retain the drug more efficiently.

Table 2. Percentage of chloroaluminum phthalocyanine (ClAlPc) incorporated into the cellulose

Sample	Incorporation / %
G1d1	47.5 ± 6.7
A2d1	87.4 ± 3.4
G3d1	44.6 ± 8.6
A3d1	41.7 ± 31.9
G1d5	25.7 ± 17.3
A2d5	41.8 ± 8.0
G1d10	27.1 ± 2.8
A2d10	34.0 ± 3.2

As expected, A2d1 showed the highest incorporation efficiency (87.4%; Table 2). The membranes grown for shorter time (A2d and G1d) have higher incorporation efficiency than A3d and G3d, and therefore they were selected for the skin permeation and retention tests. The structural characteristics of the three-dimensional network formed by cellulose nanofibrils, such as fiber density and surface area, influence on the interaction between drug molecule and polymeric matrix. Such properties influence on drug incorporation efficiency and release kinetics according to each biomaterial obtained and may be adjusted by varying the BC production process parameters. The higher amount of drug incorporated by thinner membranes (A2d and G1d) can be related to its larger surface area. In addition to this fact, a greater amount of cellulose fibers is another feature that favors higher concentrations, as observed for the membrane A2d.[40]

Skin permeation and retention *in vitro* studies

For *in vitro* permeation and skin retention, it was necessary to develop a standard calibration curve to quantify the ClAlPc present in the environment of the receiver solution (PBS pH 7.4, and ethanol 10% v/v). Serial dilutions were made with known concentrations of ClAlPc and the emission spectra were obtained under the same conditions. The curves were plotted from the emission intensities at 680 nm as a function of ClAlPc concentration. Five curves were obtained with high coefficients of determination (R^2), greater than 0.99. The calibration standard curve was obtained (y = 310357x + 218237, R^2 = 0.99) in the concentration range from 0.219 to 1.314 μg mL^{-1}.

In studies using Franz cells, the permeation profile is drawn from the quantification of ClAlPc present in the receiver solution. The tests performed for BC membranes G1d1 and A2d1 and control test (without the bacterial

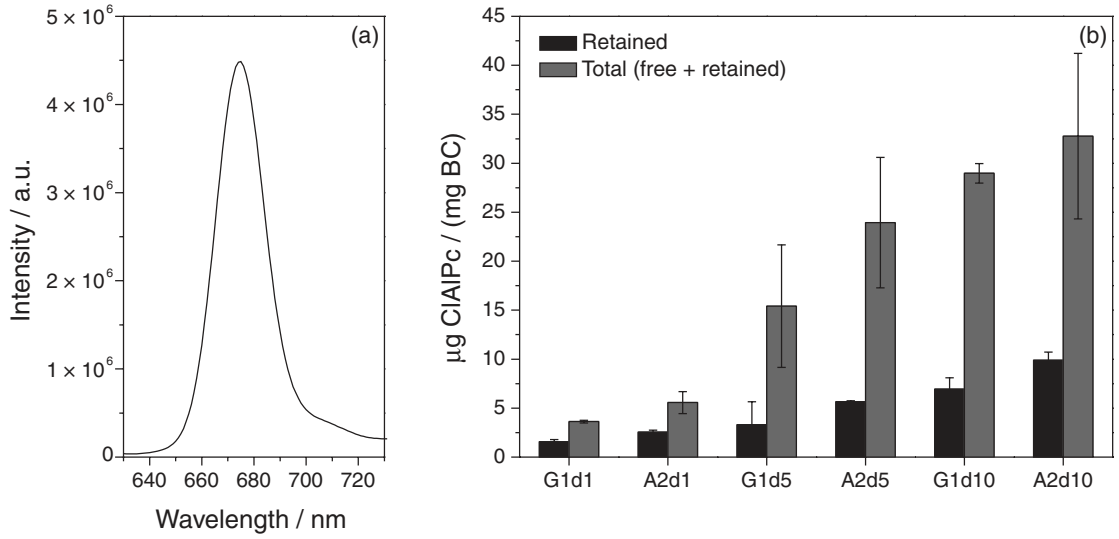

Figure 5. Chloroaluminum phthalocyanine (ClAlPc) fluorescence emission spectrum under 615 nm excitation (a); and ClAlPc retained and total (free + retained) for the thinner membranes (G1d and A2d) with different theoretical concentrations of 1, 5 and 10 μmol L^{-1} (b). Retained and total values (in μg ClAlPc *per* mg BC) for the samples are, respectively: G1d1 (1.55 and 3.62), A2d1 (2.54 and 5.56), G1d5 (3.30 and 15.42), A2d5 (5.66 and 23.93), G1d10 (6.94 and 28.97), and A2d10 (9.88 and 32.76).

cellulose matrix) showed no detectable amount of ClAlPc by fluorometry technique in the receiver solution until the period of 12 h. The absence of ClAlPc in the receiving solution may be considered positive for topical application of the photosensitizer, because it prevents its systemic absorption, which may cause a generalized photosensitization on the patient.[41,42] Stratum corneum is an efficient barrier from the external environment, controlling the flux of endogenous components outside and inside, acting as a first layer of skin with a highest lipophilic potential.[42] The effective tissue penetration is constantly associated with direct interaction between drugs and SC. For cutaneous diseases is indispensable a higher SC penetration and adequate bioaccumulation for efficient therapies and biological response.[41]

In our work, the profile of cutaneous retention in SC and skin-deep layers (epidermis + dermis = E + D) was carried out. Samples were applied topically under biomimetic conditions in a skin animal model. After hours of administration, the apparatus were dismounted and the skin treated as described in Experimental section. Tape-stripping protocols and tissue homogenization allowed determining the amount of ClAlPc penetrated and retained in skin layers. The retention profiles are shown in Figure 6 and the results are summarized in Table 3. The ClAlPc retained in the skin layers (SC and E + D) was quantified after 12 h of testing. The retention profiles of the samples A2d1 and G1d1 are illustrated in Figure 6a. ClAlPc concentrations were present in the SC 0.492 ± 0.037 μg cm^{-2} and 0.524 ± 0.032 μg cm^{-2} and in the E + D 0.408 ± 0.047 μg cm^{-2} and 0.459 ± 0.079 μg cm^{-2} to the membranes A2d1 and G1d1, respectively. The statistical analysis (ANOVA) confirmed that there is no significant difference ($p > 0.05$) between the retention profiles of the two membranes studied in both skin layers analyzed (SC and E + D). The study of ClAlPc retention in the skin layers as a function of time was conducted for the sample G1d1 for 6, 12 and 24 h (Figure 6b). The tests showed no ClAlPc in the receiver solution until the 24 h test. The retention profiles are shown in Figure 6b. ClAlPc concentrations detected in the SC for the different test times are: 6 h, 0.495 ± 0.035 μg cm^{-2}; 12 h, 0.524 ± 0.032 μg cm^{-2}; and 24 h, 0.563 ± 0.030 μg cm^{-2}. Statistical analysis showed that the profile of the 12 h test is not different from the others, i.e., there is no significant difference between 6 and 12 h and between 12 and 24 h; and 6 and 24 h tests are different. In the E + D were quantified: 6 h, 0.070 ± 0.023 μg cm^{-2}; 12 h, 0.459 ± 0.079 μg cm^{-2}; and 24 h, 0.190 ± 0.036 μg cm^{-2} (E + D). Statistical analysis showed a significant difference ($p > 0.05$) between the profiles of retention in the epidermis and dermis for the three different test times studied. Large variations in the retention values for the deeper skin layers (epidermis and dermis) were observed between the tests of 6, 12 and 24 h. The use of pig's ear skin as skin model may have led to variation in experimental results due to the enormous heterogeneity that exists between ears samples from different animals, or even in different regions of the same ear. However, it should be considered that this biological variability reflects the reality and it was possible to find a characteristic retention for the system. The use of human skin as a model[26] would be ideal for skin permeation/retention studies *in vitro*. However, this material obtained from plastic surgery presents limitations to its use, as the low availability and the need to undergo the experiment to Research Ethics Committees.[43-45] Alternatively, the animal skins, such as primate, pig, rat, guinea pig and snake, are widely used.[46] Three dimensional cultures of human cells[47]

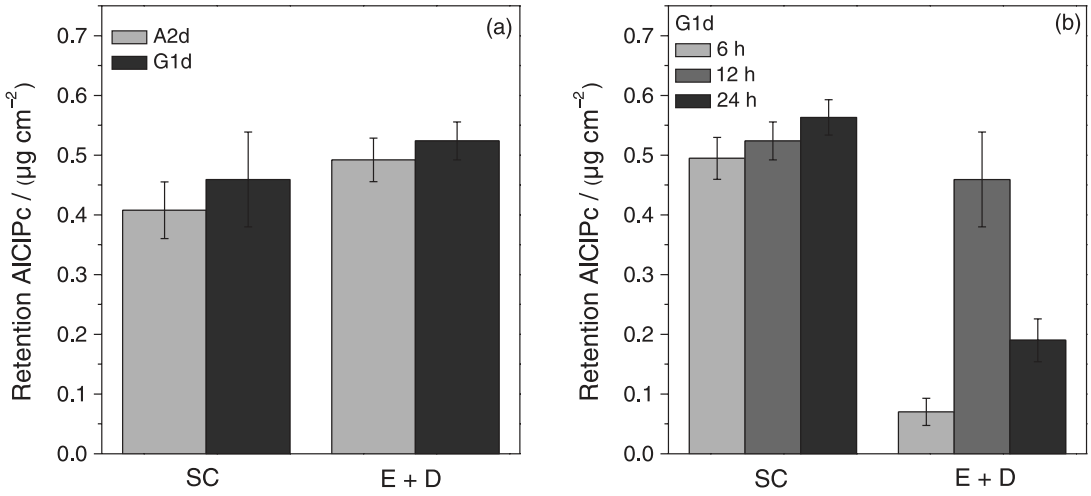

Figure 6. Penetration profiles of chloroaluminum phthalocyanine (ClAlPc) into the skin layers: epidermis + dermis (E + D) and stratum corneum (SC) for the samples A2d and G1d after 12 h (a); and G1d tested for 6, 12 and 24 h (b). Results are represented as mean ± SD (n = 5).

are also an option, however these materials are deficient in skin-associated epithelial structures (appendages), as pilosebaceous units, hair follicles and sweat glands.[48] Synthetic membranes with defined pore sizes are also employed in assays to Franz cells to reduce inter assay variation due to biological variability of the skin tissue.[49] The pig ear skin was used in this study considering the factors described above. It was also taken into account its high availability with relative ease to obtain and the low cost, once it is a by-product of the food industry. Besides being the animal model that more closely resembles histologically and biochemically to human tissue, after the primates.[46]

Table 3. Chloroaluminum phthalocyanine (ClAlPc) concentrations detected in epidermis + dermis (E + D) and stratum corneum (SC) for the samples A2d and G1d after 12 h, and for the G1d tested for 6, 12 and 24 h

Sample	time / h	SC / (μg cm^{-2})	E + D / (μg cm^{-2})
A2d	12	0.492 ± 0.037	0.408 ± 0.047
	6	0.495 ± 0.035	0.070 ± 0.023
G1d	12	0.524 ± 0.032	0.459 ± 0.079
	24	0.563 ± 0.030	0.190 ± 0.036

Mean ± SD (n = 5).

In PDT, these phenomena related to skin permeation and retention are decisive for treatment of neoplastic cells. Before laser irradiation, it is necessary that an appropriated amount of photosensitizer penetrates the SC to a better interaction with target tissues, to accumulate in malignant cells, to promote an adequate biological response and, thus, to obtain an efficient therapy. An effective delivery system for PDT by topical administration should carry the photosensitizer beyond the stratum corneum to the malignant cells present in viable layers of the epidermis.[41] A global analysis of this study permits the inference that approximately 0.5 μg cm^{-2} of ClAlPc remained in the furrows of the stratum corneum and 0.3 μg cm^{-2} in the epidermis/dermis. The drug delivery system containing a derivative of chlorine temoporfin (the synthesis and purification of Foscan® (5,10,15,20-tetra(m-hydroxyphenyl)chlorin) was carried out by Prof PhD Philippe Maillard, coordinator of the Chimie Bioorganique's Laboratoire, Institute Curie, Orsay, France) developed by Primo *et al.*[50] promoted a retention of 0.5 μg cm^{-2} drug in the stratum corneum and 0.6 μg cm^{-2} in the epidermis/dermis. Thus, the results showed an interesting alternative for delivery of photosensitizers in PDT based on bacterial cellulose, a polymer well known by a wide range of features that favors its use for biomedical applications, as mentioned above. Particularly in this case, BC-ClAlPc present advantages as a drug delivery system, as the very simple approach of preparation and the absence of cytotoxicity, according to the XTT assay.

Photophysical characterization

The singlet oxygen analysis was based on the direct detection of its luminescence at 1270 nm to measure the luminescence-decay kinetics. Lifetimes (τ) and maximum intensities observed in the decay curves are shown in Table 4. ClAlPc solution in ethanol was also evaluated for the purpose of comparing the effect of the photosensitizer free in solution. Pheophorbide A in ethanol was adopted as a standard solution for relative calculation. The lifetime values found are very close, except for the BC-ClAlPc membrane, which showed a longer lifetime. This difference may be due to the solid form of the sample.

Table 4. Fluorescence lifetimes (τ) and maximum intensities in the decay curves for the samples

Sample	τ / μs	Intensity	Increase factor
Pheophorbide A/ethanol	0.234 ± 0.011	0.040	_
ClAlPc/ethanol	0.221 ± 0.008	0.459	11.5
ClAlPc/BC	0.325 ± 0.002	0.176	4.4

BC: Bacterial cellulose; ClAlPc: chloroaluminum phthalocyanine.

Photophysical studies of BC-ClAlPc were performed for the major reactive species responsible for the destruction of tumor cells, singlet oxygen. The results shown in Table 4 are consistent with those of Siqueira-Moura *et al.*,[39] which have found similar lifetime (0.22 μs) for ClAlPc in polymeric nanocapsules. Higher luminescence intensity was obtained for BC-ClAlPc (4.4 times) in respect to the standard solution (pheophorbide A in ethanol). This compound is a derivative bacteriological hydrochloric which produces high yield of the species being studied and is widely used as a reference in spectroscopic studies.[36] Therefore, these data suggest that BC does not interfere with the production of singlet oxygen, an important condition in the PDT process.

Cytotoxicity assay (XTT cell viability assay)

Evaluation of BC-ClAlPc cytotoxicity was performed by cell viability test using Chinese hamster ovary cells (CHO-K1) because its structures and functions are common to most types of cells, i.e., the objective was to determine the basal cytotoxicity potential of BC-ClAlPc membrane.[51] The cell viability is related to the absorbance

measure. Negative control was considered 100% cell viability. Figure 7 shows the cell viability (%) expressed as mean and standard error. Cells treated with the eluate from BC-ClAlPc membrane showed 32% of lower cell viability than negative control (without any treatment). Therefore, cell viability of the BC-ClAlPc membrane is not significantly different from NC ($p > 0.05$; Dunnett). Thus, the BC-ClAlPc membrane does not significantly affect cell viability, being non-cytotoxic.

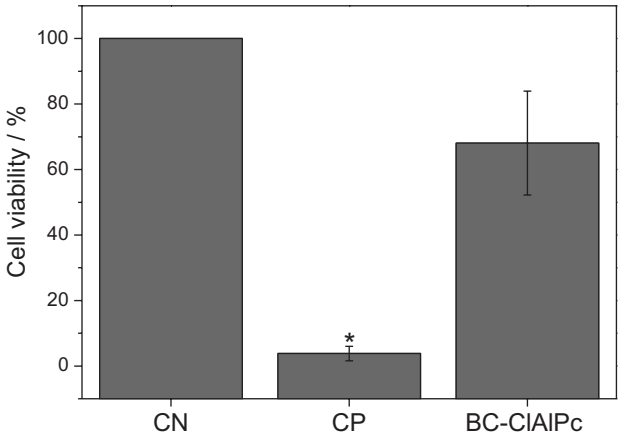

Figure 7. Cell viability obtained from XTT test for negative control (NC), positive control (PC) and bacterial cellulose (BC)-chloroaluminum phthalocyanine (ClAlPc) membrane. *Indicates statistically significant difference from the negative control. Mean ± SE ($p < 0.05$, Dunnett).

For a safe use in humans, biomaterials should not present cytotoxic effects. The cytotoxicity potential of pure BC was already evaluated by Saska *et al.*,[52] which demonstrated absence of *in vitro* cytotoxicity effects of BC membranes. In the present study, cytotoxicity assay demonstrated that BC-ClAlPc membrane was non-cytotoxic in CHO-K1 cells. The non-cytotoxic profile is an essential consideration when developing a material for safe use in a biomedical application. Thus, cytotoxicity assay is the first step toward ensuring the biocompatibility of a biomaterial. This fact combined with the skin permeation/retention profiles are indicators of the strong potential of BC-ClAlPc membranes as a topical drug delivery system for PDT.

Conclusions

The study showed the feasibility of using BC as a matrix for incorporation and controlled release of photosensitizers. BC membranes with different properties were obtained by varying the bacterial strains and production times. The interaction between the BC and ClAlPc was confirmed by FTIR spectra. The results showed that the structural properties of membranes (such as thickness, fibers amount, surface area) correlates with the drug incorporation efficiency. The permeation/retention profiles observed for BC-ClAlPc confirm the possibility of using this system in topical administration in the process of PDT. The photophysical properties of ClAlPc are not affected after its incorporation in BC membranes. Moreover, these membranes demonstrated no *in vitro* cytotoxicity effects, suggesting their potential for safe biological use.

Acknowledgments

This study was supported by the Brazilian agency FAPESP (process No. 2011/15759-7). Rede CON-NANO-CAPES awarded a fellowship to Maristela de F. S. Peres.

References

1. Seigneuric, R.; Markey, L.; Nuyten, D. S. A.; Dubernet, C.; Evelo, C. T. A.; Finot, E.; Garrido, C; *Curr. Mol. Med.* **2010**, *10*, 640.
2. Wilson, B. C. In *Photon-Based Nanoscience and Nanobiotechnology*; Dubowski, J.; Tanev, S., eds.; Springer: Dordrecht, 2006, ch. 7.
3. Barreto, J. A.; O'Malley, W.; Kubeil, M.; Graham, B.; Stephan, H.; Spiccia, L.; *Adv. Mater. (Weinheim, Ger.)* **2011**, *23*, H18.
4. Dolmans, D. E.; Fukumura, D.; Jain, R. K.; *Nat. Rev. Cancer* **2003**, *3*, 380.
5. Trauner, K. B.; Gandour-Edwards, R.; Bamberg, M.; Shortkroff, S.; Sledge, C.; Hasan, T.; *Photochem. Photobiol.* **1998**, *67*, 133.
6. Mitra, A.; Stables, G. I.; *Photodiagn. Photodyn. Ther.* **2006**, *3*, 116.
7. Jori, G.; Fabris, C.; Soncin, M.; Ferro, S.; Coppellotti, O.; Dei, D.; Fantetti, L.; Chiti, G.; Roncucci, G.; *Lasers Surg. Med.* **2006**, *38*, 468.
8. Dai, T.; Huang, Y. Y.; Hamblin, M. R.; *Photodiagn. Photodyn. Ther.* **2009**, *6*, 170.
9. Agostinis, P.; Berg, K.; Cengel, K. A.; Foster, T. H.; Girotti, A. W.; Gollnick, S. O.; Hahn, S. M.; Hamblin, M. R.; Juzeniene, A.; Kessel, D.; Korbelik, M.; Moan, J.; Mroz, P.; Nowis, D.; Piette, J.; Wilson, B. C.; Golab, J.; *Ca-Cancer J. Clin.* **2011**, *61*, 250.
10. Castano, A. P.; Demidova, T. N.; Hamblin, M. R.; *Photodiagn. Photodyn. Ther.* **2004**, *1*, 279.
11. Konan, Y. N.; Gurny, R.; Allémann, E; *J. Photochem. Photobiol., B* **2002**, *66*, 89.
12. Ernsting, M. J.; Murakami, M.; Roy, A.; Li, S. D.; *J. Controlled Release* **2013**, *172*, 782.
13. Yamagata, T.; Morishita, M.; Kavimandan, N. J.; Nakamura, K.; Fukuoka, Y.; Takayama, K.; Peppas, N. A.; *J. Controlled Release* **2006**, *112*, 343.

14. Lancer, R.; *Acc. Chem. Res*. **1993**, *26*, 537.
15. McHugh, A. J.; *J. Controlled Release* **2005**, *109*, 211.
16. Sugibayashi, K.; Morimoto, Y.; *J. Controlled Release* **1994**, *29*, 177.
17. Jawahar, N.; Meyyanathan, S.; *Int. J. Health Allied Sci.* **2012**, *1*, 217.
18. Rios, M.; *Pharm. Technol.* **2005**, *29*, 42.
19. Percoraro, E.; Manzani, D.; Messaddeq, Y.; Ribeiro, S. J. L. In *Monomers, Polymers and Composites from Renewable Resources*; Belgacem M. N.; Gandini, A., eds.; Elsevier: Amsterdam, 2008, ch. 17.
20. Czaja, W. K.; Young, D. J.; Kawecki, M.; Brown, R. M.; *Biomacromolecules* **2007**, *8*, 1.
21. Amin, M. C. I. M.; Ahmad, N.; Halib, N.; Ahmad, I.; *Carbohydr. Polym*. **2012**, *88*, 465.
22. Torres, F. G.; Commeaux, S.; Troncoso, O. P.; *J. Funct. Biomater*. **2012**, *3*, 864.
23. Huang, L.; Chen, X.; Nguyen, T. X.; Tang, H.; Zhang, L.; Yang, G.; *J. Mater. Chem. B* **2013**, *1*, 2976.
24. Bodhibukkana, C.; Srichana, T.; Kaewnopparat, S.; Tangthong, N.; Bouking, P.; Martin, G. P.; Suedee, R.; *J. Controlled Release* **2006**, *113*, 43.
25. Stoica-Guzun, A.; Stroescu, M.; Tache, F.; Zaharescu T.; Grosu, E.; *Nucl. Instrum. Methods Phys. Res., Sect. B* **2007**, *265*, 434.
26. Trovatti, E.; Freire, C. S. R.; Pinto, P. C.; Almeida, I. F.; Costa, P.; Silvestre, A. J. D.; Neto, C. P.; Rosado, C.; *Int. J. Pharm. (Amsterdam, Neth.)* **2012**, *435*, 83.
27. Almeida, I. F.; Pereira, T.; Silva, N. H.; Gomes, F. P.; Silvestre, A. J.; Freire, C. S.; Lobo, J. M. S.; Costa, P. C.; *Eur. J. Pharm. Biopharm*. **2014**, *86*, 332.
28. Padula, C.; Colombo, G.; Nicoli, S.; Catellani, P. L.; Massimo, G.; Santi, P.; *J. Controlled Releas*e **2003**, *88*, 277.
29. Nigoghossian, K.; Peres, M. F. S.; Primo, F. L.; Tedesco, A. C.; Pecoraro, E.; Messaddeq, Y.; Ribeiro, S. J. L.; *Colloids Interface Sci. Commun.* **2014**, *2*, 6.
30. Schmitt, F.; Lagopoulos, L.; Käuper, P.; Rossi, N.; Busso, N.; Barge, J.; Wagnières, G.; Laue, C.; Wandrey, C.; Juillerat-Jeanneret, L.; *J. Controlled Release* **2010**, *144*, 242.
31. Drogat, N.; Granet, R.; Le Morvan, C.; Bégaud-Grimaud, G.; Krausz, P.; Sol, V.; *Bioorg. Med. Chem. Lett.* **2012**, *22*, 3648.
32. Bionext Produtos Biotecnológicos Ltda. (Brazil). Farah, L. F. X.; Podlech, P.A.S.; Archanjo, C. R.; Coral., L. A.; US 2009/0017506.
33. Siqueira-Moura, M. P.; Primo, F. L.; Peti, A. P. F.; Tedesco, A. C.; *Pharmazie* **2010**, *65*, 9.
34. Sartorelli, P.; Andersen, H. R.; Angerer, J.; Corish, J.; Drexler, H.; Göen, T.; Griffin, P.; Hotchkiss, S. A.; Larese, F.; Montomoli, L.; Perkins, J.; Schmelz, M.; van de Sandt, J.; Williams, F.; *Environ. Toxicol. Pharmacol.* **2000**, *8*, 133.
35. Godin, B.; Touitou, E.; *Adv. Drug. Delivery Rev.* **2007**, *59*, 1152.
36. Krasnovsky Jr, A. A.; Neverov, K. V.; Egorov, S. Y.; Roeder, B.; Levald, T.; *J. Photochem. Photobiol., B* **1990**, *5*, 245.
37. Silva, W. J.; Seneviratne, J.; Parahitiyawa, N.; Rosa, E. A. R.; Samaranayake, L. P.; del Bel Cury, A. A.; *Braz. Dent. J.* **2008**, *19*, 364-369.
38. Basova, T. V.; Kiselev, V. G.; Plyashkevich, V. A.; Cheblakov, P. B.; Latteyer, F.; Peisert, H.; Chassè, T.; *Chem. Phys.* **2011**, *380*, 40.
39. Siqueira-Moura, M. P.; Primo, F. L.; Espreafico, E. M.; Tedesco, A. C.; *Mater. Sci. Eng., C* **2013**, *33*, 1744.
40. Rezaei, A.; Nasirpour, A.; Fathi, M.; *Compr. Rev. Food Sci. Food Saf.* **2015**, *14*, 269.
41. Rossetti, F. C.; Lopes, L. B.; Carollo, A. R. H.; Thomazini, J. A.; Tedesco, A. C.; Bentley, M. V. L. B.; *J. Controlled Release* **2011**, *155*, 400.
42. Shah, V. P. In *Drug Permeation Enhancement - Theory and Applications*; Hsieh, D. S., ed.; Marcel Dekker: New York, 1994, ch. 2.
43. Schmook, F. P.; Meingassner; J. G.; Billich, A.; *Int. J. Pharm. (Amsterdam, Neth.)* **2001**, *215*, 51.
44. Rigg, P. C.; Barry, B. W.; *J. Invest. Dermatol*. **1990**, *94*, 235.
45. Baby, A. R.; Haroutiounian Filho, C. A.; Sarruf, F. D.; Tavante Júnior, C. R.; Pinto, C. A. S. O.; Zague, V.; Arêas, E. P. G.; Kaneko, T. M.; Velasco. M. V. R.; *Rev. Bras. Cienc. Farm.* **2008**, *44*, 233.
46. Godin, B.; Touitou, E.; *Adv. Drug. Delivery Rev.* **2007**, *59*, 1152.
47. Primo, F. L.; Reis, M. B. C.; Porcionatto, M. A.; Tedesco, A. C.; *Curr. Med. Chem.* **2011**, *18*, 3376.
48. Netzlaff, F.; Lehr, C. M.; Wertz, P. W.; Schaefer, U. F.; *Eur. J. Pharm. Biopharm*. **2005**, *60*, 167.
49. Coulman, S. A.; Barrow, D.; Anstey, A.; Gateley, C.; Morrissey, A.; Wilke, N.; Allender, C.; Brain, K.; Birchall, J. C.; *Curr. Drug Delivery* **2006**, *3*, 65.
50. Primo, F. L.; Michieleto, L.; Rodrigues, M. A. M.; Macaroff, P. P.; Morais, P. C.; Lacava, Z. G. M.; Bentley, M. V. L. B.; Tedesco, A. C.; *J. Magn. Magn. Mater*. **2007**, *311*, 354.
51. Ekwall, B.; Silano, V.; Paganuzzi-Stammati, A.; Zucco, F. In *Short-Term Toxicity Tests for Non-Genotoxic Effects*; Bourdeau, P.; Sommers, E.; Richardson, G. M.; Hickman, J. R., eds.; Wiley: Chichester, 1990, 7, 75.
52. Saska, S.; Scarel-Caminaga, R. M.; Teixeira, L. N.; Franchi, L. P.; dos Santos, R. A.; Gaspar, A. M. M.; Oliveira, P. T.; Rosa, A. L.; Takahashi, C. S.; Messaddeq, Y.; Ribeiro, S. J. L.; Marchetto, R.; *J. Mater. Sci: Mater.: Med* **2012**, *23*, 225

Submitted: December 29, 2015
Published online: March 17, 2016

FAPESP has sponsored the publication of this article.